Liquid Crystals
Publication details, including instructions for authors and subscription information:
http://www.informaworld.com/smpp/title~content=t713926090

A study on the effect of carboxylate ester and thioester linking groups in ferroelectric liquid crystal dimers

S. -L. Wu Corresponding author[a]; S. Senthil[a]
[a] Department of Chemical Engineering, Tatung University, Taiwan, ROC

Online publication date: 12 May 2010

To cite this Article Wu Corresponding author, S. -L. and Senthil, S.(2004) 'A study on the effect of carboxylate ester and thioester linking groups in ferroelectric liquid crystal dimers', Liquid Crystals, 31: 12, 1573 — 1579
To link to this Article: DOI: 10.1080/02678290412331273307
URL: http://dx.doi.org/10.1080/02678290412331273307

LIQUID CRYSTALS, VOL. 31, NO. 12, DECEMBER 2004, 1573–1579

A study on the effect of carboxylate ester and thioester linking groups in ferroelectric liquid crystal dimers

S.-L. WU* and S. SENTHIL

Department of Chemical Engineering, Tatung University, 40 Chungshan N. Rd., 3rd sec., Taipei 104, Taiwan, ROC

(*Received 4 February 2004; accepted 2 April 2004*)

Two series of symmetrical liquid crystal twins possessing a chiral centre at the inner side of the molecules were synthesized and characterized. Structural effects on the mesomorphic and physical properties were investigated in terms of (a) variation of carboxylate and thioester groups linking the spacer and core, (b) variation in achiral chain length between two mesogenic units. The mesomorphic investigation reveals that these compounds exhibit a BP, N*, SmA* and SmC* mesophase sequence for the BDPNP series, and a SmA and SmC* sequence for the ABPNTP-*n* series. The $\mathbf{P}_s$ values were measured and a largest of 38.5 nC cm^{-2} was observed for ABPNTP-12.

1. Introduction

The fascinating behaviour of liquid crystal dimers, in which mesogenic groups are linked by a flexible spacer, is usually associated with the major dependence of the properties on the parity [1], length of the spacer [2] and chemical constitution [3]. Liquid crystals with a very wide SmC* phase are very useful materials as they may give long operational temperature ranges [4], and are found to be useful in binary mixtures [5, 6]. In particular, the thiobenzoate group at the interface of the core and spacer are reported to enhance the SmC* phase width [7, 8]. This group shows an interesting suppression of many smectic polymorphisms, and enhances the SmC* mesophase range [9–11]. It is generally acknowledged to be due to the differences of dipole moments between carboxylate and thioester, causing a large change in dielectric anisotropy [12, 13]. The difference in bend angles of the –COO– and –COS– groups generates considerable dipole change, leading to a large variation in mesomorphic characteristics [14, 15].

In this present investigation, we decided to study the effect on mesomorphic and physical properties of –COO– and –COS– linkages in liquid crystal twins. Generally, in liquid crystal twins, the spacer chain attached to the chiral centre produces large variations on both mesomorphic and physical properties [16]. Hence we have designed two series of LC twins in which one series has a –COO– linkage and other a –COS– linkage nearest to the chiral centre at the inner side of the molecule. The formula of the target molecule is depicted below.

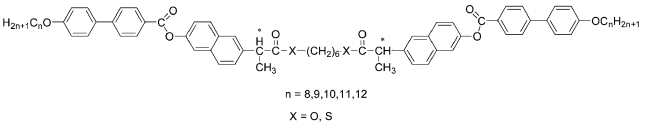

Formula.

2. Experimental

2.1. *Characterization of materials*

The chemical structures of intermediates and target materials were analysed by nuclear magnetic resonance spectroscopy using a Jeol EX-400 FTNMR spectrometer. Purity was checked by thin layer chromatography and further confirmed by elemental analysis using a Perkin-Elmer 2400 elemental analyser. Transition temperatures and phase transition enthalpies were determined by differential scanning calorimetry using a Perkin-Elmer DSC7 calorimeter at a heating rate of 5°C min^{-1}. Mesophases were principally identified by the microscope texture of the materials sandwiched between two glass plates by polarizing optical microscopy, using a Nikon Microphot-FXA in conjunction with an Instec HS1 hot stage.

The physical properties of the ferroelectric phase for the materials were measured in antiparallel aligned cells purchased from E.H.C Co. Japan. The spontaneous polarization $\mathbf{P}_s$ was measured by a triangular

*Author for correspondence; e-mail: slwu@ttu.edu.tw

Liquid Crystals ISSN 0267-8292 print/ISSN 1366-5855 online © 2004 Taylor & Francis Ltd
http://www.tandf.co.uk/journals
DOI: 10.1080/02678290412331273307

wave method [17]. The measurement of optical transmittance versus applied electric field was conducted using a He-Ne laser (5 mW, 632.8 nm) as a probe beam [18, 19] passing through the cell between crossed polarizers, whose axes were parallel and perpendicular to the smectic layer normal, with a photodiode detector. The signals were detected with a HP54502A digital oscilloscope. The voltage applied to the cell was produced by an arbitrary wave form generator (AG1200) and amplified by a homemade power preamplifier.

2.2. *General synthetic procedure*

The starting chiral material was esterified with 1,6-hexanediol and 1,6-hexanedithiol in the presence of *N*,*N*-dicyclohexylcarbodiimide (DCC) and 4-(dimethylamino)pyridine (DMAP) to produce the ester, hexyl bis[(*S*)-2-(6-methoxy-2-naphthyl)propionate]. The methoxy group of the diester was demethylated using BBr_3 and the resulting dihydroxy compound further esterified with 4-(4-alkoxyphenyl)benzoic acid using DCC and DMAP to obtain the target dimers. All the intermediates and final products were purified by column chromatography on silica gel, using dichloromethane as eluent. The synthetic procedures for the target compounds were carried out as outlined in the scheme.

2.3. *Preparation of materials*

The chiral starting material, (*S*)-2-(6-methoxy-2-naphthyl)propionic acid, 1,6-hexanediol and 1,6-hexanedithiol were purchased from Tokyo chemical Industry (TCI), Japan, with purity greater than 99%. Thin layer chromatography was performed with TLC sheets coated with silica; spots were detected by UV irradiation. Silica gel (MN Kieselgel 60, 70–230mesh) was used for column chromatography. The organic solvent dichloromethane was purified by treatment with CaH_2 and distilled before use. The spectral data are in accordance with expected molecular structure. A

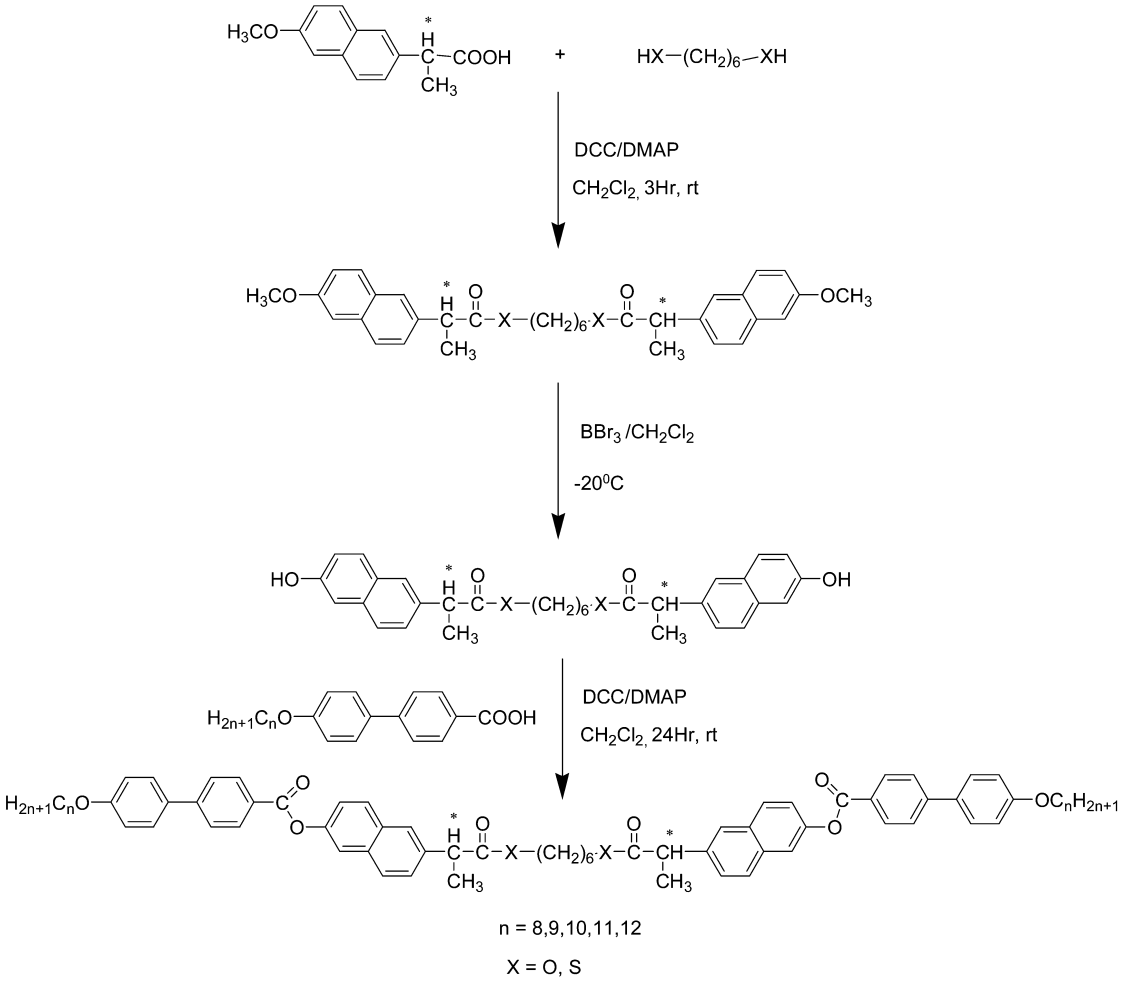

Scheme. Synthesis of the dimers.

representative synthetic procedure and analytical data are provided below.

2.3.1. *Hexyl bis[(S)-2-(6-methoxy-2-naphthyl)-propionate]*

(*S*)-2-(6-methoxy-2-naphthyl)propionic acid (2.53 g, 0.011 mol), 1,6-hexanediol (0.59 g, 0.005 mol) and DMAP (0.12 g, 0.001 mol) were mixed in dry dichloromethane (25 ml). DCC (2.68 g, 0.013 mol) was then added and the resulting mixture stirred at room temperature for 3 h. Precipitated materials were removed by filtration. The solution was washed with 5% acetic acid (3 × 50 ml) and saturated NaCl (3 × 50ml), followed by water. The organic layer was dried over anhydrous $MgSO_4$ and filtered; the solvent removed under reduced pressure. The product was purified by column chromatography using dichloromethane as eluent, and recrystallized from ethanol giving a white solid; yield 3.5 g (90%). ^{1}H NMR ($CDCl_3$, δ ppm): 1.07 (d, 3H, *CHC**H**$_3$), 1.1–1.19 (m, 2H, C**H**$_2$), 1.5–1.58 (m, 2H, OCH$_2$C**H**$_2$), 3.82 (q, 1H, *C**H**), 3.85 (s, 3H, OC**H**$_3$), 4.05 (t, 2H, OC**H**$_2$), 7.09–7.69 (m, 6H, Ar**H**).

2.3.2. *Hexyl bis[(S)-2-(6-methoxy-2-naphthyl)-thiopropionate]*

(*S*)-2-(6-methoxy-2-naphthyl)propionic acid (2.53 g, 0.011 mol), 1,6-hexanethiol (0.59 g, 0.005 mol) and DMAP (0.12 g, 0.001 mol) were mixed in dry dichloromethane (25 ml). DCC (2.68 g, 0.013 mol) was then added and the resulting mixture stirred at room temperature for 3 h. Precipitated materials were removed by filtration. The solution was washed with 5% acetic acid (3 × 50 ml) and satd. NaCl (3 × 50ml), followed by water. The organic layer was dried over anhydrous $MgSO_4$ and filtered; the solvent was removed under reduced pressure. The product was purified by column chromatography using dichloromethane as eluent and recrystallized from ethanol giving a white solid; yield 3.5 g (90%). ^{1}H NMR ($CDCl_3$, δ ppm): 1.07 (d, 3H, *CHC**H**$_3$), 1.1–1.19 (m, 2H, C**H**$_2$), 1.5–1.58 (m, 2H, OCH$_2$C**H**$_2$), 3.85 (s, 3H, OC**H**$_3$), 2.68 (t, 4H, SC**H**$_2$), 3.94 (t, 5H, OC**H**$_2$,*C**H**), 7.09–7.69(m, 6H, Ar**H**).

2.3.3. *Hexyl bis[(S)-2-(6-hydroxy-2-naphthyl)-propionate]*

Hexyl bis[(*S*)-2-(6-methoxy-2-naphthyl)propionate] (2.7 g, 0.005 mol) was dissolved in dry dichloromethane (25 ml) and cooled to −20°C. BBr_3 (2.5 ml) was added slowly under an inert atmosphere with stirring; the reaction was continuously followed by TLC. Dichloromethane (200 ml) was added soon after the completion of reaction. The solution was poured into ice-cooled satd. NH_4Cl solution (250 ml). The mixture was stirred and the organic layer was washed with satd. NaCl solution (3 × 200 ml), water (3 × 200 ml); it was then dried over anhydrous $MgSO_4$, filtered and the solvent was removed under reduced pressure. The product was purified by column chromatography using a dichloromethane/ethyl acetate (5/1) mixture, to give a white solid; yield 1.9 g (75%). ^{1}H NMR (DMSO-d_6, δ ppm): 1.06 (d, 3H, *CHC**H**$_3$), 1.17–1.20 (m, 2H, C**H**$_2$), 1.32–1.43 (m, 2H, C**H**$_2$), 3.83(q, 1H, *C**H**), 4.05 (t, 2H, OC**H**$_2$), 7.02–7.58 (m, 6H, Ar**H**), 9.72 (s, 1H, O**H**).

2.3.4. *Hexyl bis[(S)-2-(6-hydroxy-2-naphthyl)-thiopropionate]*

Hexyl bis[(*S*)-2-(6-methoxy-2-naphthyl)thiopropionate] (2.7 g, 0.005 mol) was dissolved in dry dichloromethane (25 ml) and cooled to −20°C. BBr_3 (2.5 ml) was added slowly under an inert atmosphere with stirring. The reaction was continuously followed by TLC. Dichloromethane (200 ml) was added soon after the completion of reaction. The solution was poured into ice-cooled satd. NH_4Cl solution (250 ml). The mixture was stirred and the organic layer washed with satd. NaCl solution (3X200ml), water (3 × 200 ml); it was then dried over anhydrous $MgSO_4$, filtered and the solvent removed under reduced pressure. The product was purified by column chromatography using dichloromethane/ethyl acetate (5/1) mixture, to give a white solid; yield 1.9 g (75%). ^{1}H NMR (DMSO-d_6, δ ppm): 1.06 (d, 3H, *CHC**H**$_3$), 1.17–1.20 (m, 2H, C**H**$_2$), 1.32–1.43 (m, 2H, C**H**$_2$), 2.79 (t, 4H, SC**H**$_2$), 3.98 (t, 5H, OC**H**$_2$, *C**H**), 7.02–7.58 (m, 6H, Ar**H**), 9.72 (s, 1H, O**H**).

2.3.5. *Hexyl bis{(S)-2-[6-(4-octyloxyphenylbenzoyloxy)-2-naphthyl]propionate} (ABPNP-8)*

Hexyl bis[(S)-2-(6-hydroxy-2-naphthyl)propionate] (0.5 g, 0.001 mol), 4-(4-octyloxyphenyl)benzoic acid (0.85 g, 0.0025 mol) and DMAP (1.2 g) were mixed in dry dichloromethane (25 ml). DCC (0.52 g, 0.0025 mol) was then added and the resulting mixture stirred at room temperature for one day. Precipitated materials were removed by filtration, and the solvent removed under reduced pressure. The product was purified by column chromatography using dichloromethane as eluent, and recrystallized from ethanol giving white solid; yield 1 g (70%). ^{1}H NMR ($CDCl_3$, δ ppm): 1.54 (d, 3H, *CHC**H**$_3$), 0.86–1.27 (m, 19H, C**H**$_2$), 1.8–1.82 (m, 4H, CH$_2$C**H**$_2$), 3.73 (q, 1H, *C**H**), 4.01 (t, 4H, OC**H**$_2$), 6.97–8.26 (m, 10H, ArH). Elemental analysis:

calculated for $C_{74}H_{82}O_{10}$. C 78.89, H 7.64; found. C 78.78, H 7.63%. A similar procedure was adopted for the preparation of other compounds in the series by reaction of the corresponding acids.

2.3.6. *Hexyl bis{(S)-2-[6-(4-octyloxyphenylbenzoyloxy)-2-naphthyl] thiopropionate} (ABPNTP-8)*

Hexyl bis[(*S*)-2-(6-hydroxy-2-naphthyl)thiopropionate] (0.5 g, 0.001 mol), 4-(4-octyloxyphenyl)benzoic acid (0.85 g, 0.0025 mol) and DMAP (1.2 g) were mixed in dry dichloromethane (25 ml). DCC (0.52 g, 0.0025 mol) was added and the resulting mixture stirred at room temperature for one day. Precipitated materials were removed by filtration, and the solvent removed under reduced pressure. The product was purified by column chromatography using dichloromethane as eluent and recrystallized from ethanol giving a white solid; yield 1 g (70%). ^{1}H NMR ($CDCl_3$, δ ppm): 1.54 (d, 3H, *CHC**H**$_3$), 0.86–1.27 (m, 19H, C**H**$_2$), 2.8 (t, 4H, SC**H**$_2$), 4.01 (t, 5H, OC**H**$_2$, *C**H**), 6.97–8.26 (m, 10H, ArH). Elemental analysis: calculated for $C_{74}H_{82}O_8S_2$ C 76.39, H 7.10; found. C 77.18, H 7.53%. A similar procedure was adopted for the preparation of other compounds in the series by reaction of the corresponding acids.

3. Results and discussion

3.1. *Mesomorphic properties*

The mesophases and their corresponding phase transition temperatures observed are given in the table 1. The ABPNP-*n* series of compounds exhibit BP_I, BP_{II}, N*, SmA* and SmC* textures, whereas the ABPNTP-*n* series exhibit only SmA* and SmC* textures during cooling from the isotropic state. All the observed mesophases were identified against reported textures [20]. The BP_I phase formed blue–yellow clean platelets, and the BP_{II} phase was identified by blue–pale brown coloured wrinkled platelets. The N* phase was recognized by its paramorphotic texture and it was further confirmed by observing a flash on subjecting it to mechanical stress. The SmA* phase was identified by its optical texture, which showed a co-existence of clean focal-conic and homeotropic textures in the ABPNP-*n* series. The ABPNTP-*n* series also showed the SmA* focal-conic texture. The SmC* phase in the ABPNP-*n* series was characterized by the formation of broken focal-conic texture, whereas for the ABPNTP-*n* series a paramorphotic broken focal-conic texture was observed.

DSC thermograms of all compounds in the ABPNP-*n* series exhibit three monotropic endotherms corresponding to I–BP, BP–N* transitions and crystallization. The enthalpy of the SmA*–SmC* phase transition was too small to measure, but the enthalpy of the I–BP, BP–N* and N*–SmA* transitions are significant. A phase diagram as a function of transition temperatures for the ABPNP-*n* series is shown in figure 1. It can be seen that isotropic, BP and N* phase transition temperatures decrease with increasing achiral chain length. But the transition temperature of the SmC* phase is changed very little with increasing

Table 1. Mesophases and transition temperatures (°C) of the liquid crystal dimers; enthalpies are shown in italics.

Compound	m.p.	Cr		SmX*		SmC*		SmA*		N*		BP_I		BP_{II}		I
	128.25	•	69.89	•	88.96	•	135.25	•	181.27	•	187.81	•	189.96	•	192.1	•
ABPNP-8	*39.77*		*7.016*		[a]		[a]		*6.775*		*0.835*		[a]		*1.381*	
	136.69	•	80.52	•	89.63	•	142.9	•	177.26	•	182.2	•	186.05	•	188.22	•
ABPNP-9	*33.67*		*14.49*		[a]		[a]		*1.117*		*0.248*		[a]		*1.117*	
	132.04	•	71.18	•	90.52	•	143.0	•	178.86	•	181.21	•	182.09	•	184.43	•
ABPNP-10	*29.46*		*8.705*		[a]		[a]		*1.21*		*0.219*		[a]		*1.297*	
	134.57	•	81.37	•	87.0	•	142.0	•	172.91	•	174.93	•	176.02	•	177.76	•
ABPNP-11	*27.18*		*22.6*		[a]		[a]		*1.358*		*0.758*		[a]		*0.258*	
	135.52	•	87.26	•	93.0	•	140.23	•	169.28	•	171.7	•	172.1	•	174.56	•
ABPNP-12	*26.35*		*21.4*		[a]		[a]		*1.208*		*0.523*		[a]		*0.203*	
	170.01	•	117.64		–	•	152.3		–		–		–	•	187.62	•
ABPNTP-8	*30.43*		*23.62*				[a]								*11.97*	
	172.06	•	132.27		–	•	162.4		–		–		–	•	180.92	•
ABPNTP-9	*32.55*		*27.59*				[a]								*9.754*	
	161.14	•	126.21		–	•	163.28		–		–		–	•	174.68	•
ABPNTP-10	*27.6*		*26.28*				*0.783*								*8.378*	
	151.26	•	115.77		–	•	163.01		–		–		–	•	169.92	•
ABPNTP-11	*27.26*		*28.75*				*2.806*								*10.68*	
	153.6	•	115.11		–	•	158.16		–		–		–	•	164.31	•
ABPNTP-12	*15.97*		*7.866*				*1.519*								*4.136*	

[a]Enthalpies were too small to calculate by the instrument.

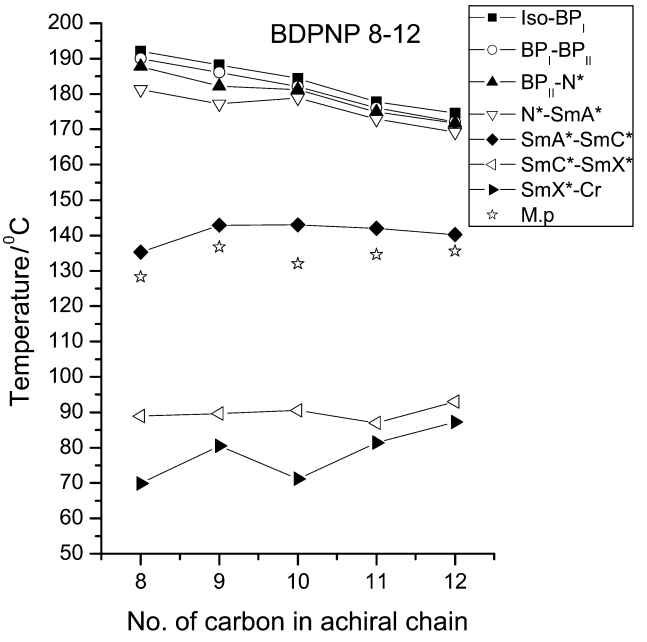

Figure 1. Transition temperature as a function of spacer length on cooling for the ABPNP-*n* series of compounds.

achiral chain length. The phase diagram also shows that the increase in achiral chain length produces no significant change in SmC* phase range in a given series.

A phase diagram for the ABPNTP-*n* series of compounds is shown in figure 2, and shows that, the clearing temperature decreases linearly by about 5 degrees for every additional carbon in the achiral chain. It is interesting to note that SmC* transition temperatures increases on increasing the chain length. Thus SmA* phase ranges decrease with increasing carbons, remaining constant after 10 carbons. Figure 2 also shows that the SmC* range is the same for 8 and 9 carbons, but increases significantly with further increase of carbons in the achiral chain. In general, the replacement of an oxygen atom by sulphur in the internal linking group produces significant changes in mesomorphic characteristics, mesophase stability and transition temperatures.

3.2. *Spontaneous polarization and tilt angle*

The magnitude of spontaneous polarizations ($\mathbf{P}_s$ values) for the ABPNP-*n* and ABPNPT-*n* series of compounds are plotted in figures 3 and 4, respectively. It is interesting to note that the largest $\mathbf{P}_s$ values among all the compounds was observed in ABPNTP-12 ($38.2\,\mathrm{nC\,cm^{-2}}$) which has a thioester linkage. A plot of $\mathbf{P}_s$ against achiral chain length at 20°C below the respective SmA*–SmC* transition temperatures is shown in figure 5. The $\mathbf{P}_s$ value increases considerably from the octyloxy to nonyloxy derivative in both series, and then decreases by small amount up to the undecyloxy derivative. Further increase of achiral chain length produces an increase in the ABPNTP-*n* series and a decrease in the ABPNP-*n* series. It can also be seen that a considerable increase in $\mathbf{P}_s$ value is seen for the thio-ester linking group over the carboxylic-ester linkage. In the case of low molecular mass analogues [21, 22] with same core unit, there is a pronounced

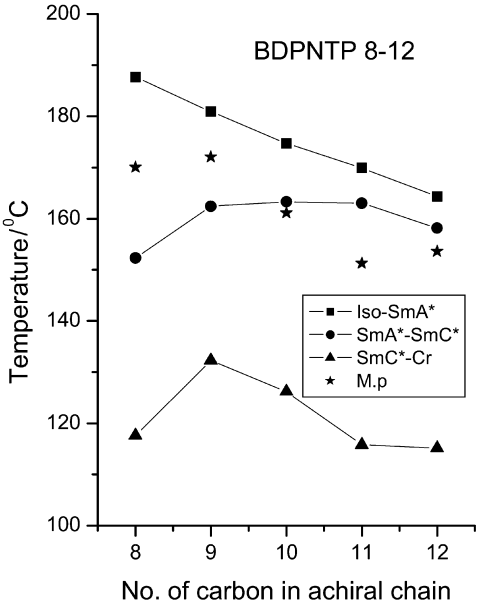

Figure 2. Transition temperature as a function of spacer length on cooling for the ABPNTP-*n* series of compounds.

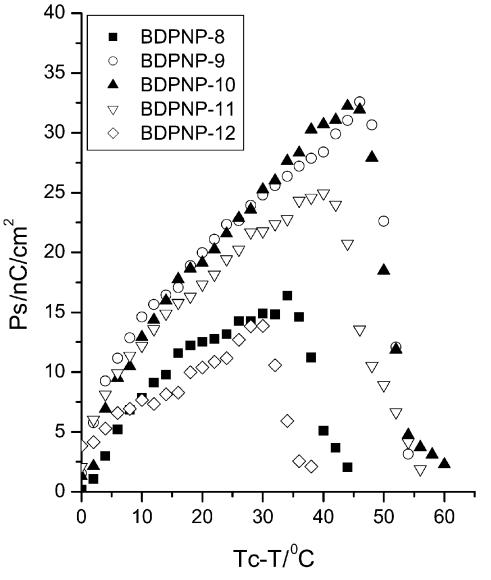

Figure 3. Spontaneous polarization as a function of temperature for the ABPNP-*n* series of compounds.

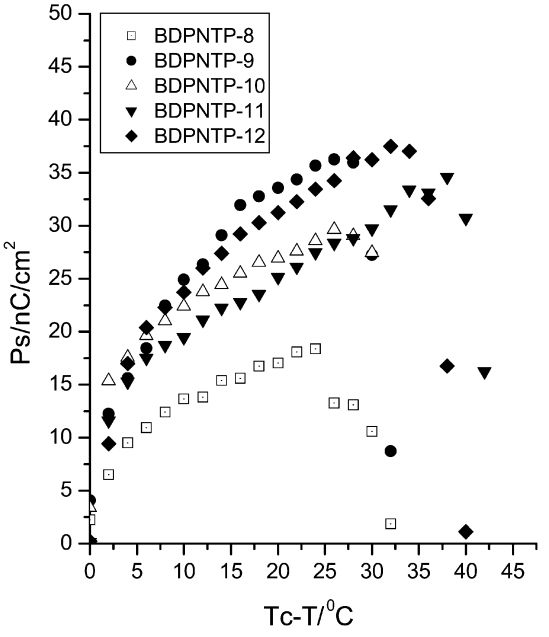

Figure 4. Spontaneous polarization as a function of temperature for the ABPNTP-*n* series of compounds.

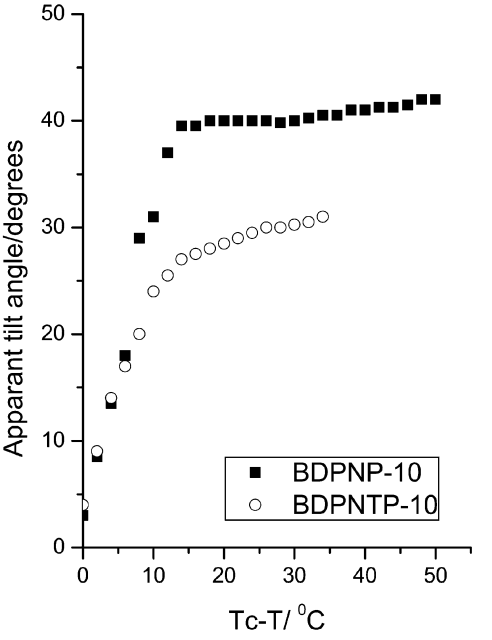

Figure 6. Apparent tilt angle as a function of temperature measured in the SmC* phase of ABPNP-10 (■) and ABPNTP-10 (○).

effect of a two-fold increase in $\mathbf{P}_s$ value on replacing the carboxylate by a thio-ester unit. But in the case of the dimers, the only significant change of $\mathbf{P}_s$ value is with the changing linking group. This is presumably because the change of linking groups at the inner side of the molecule has less effect on the rotational freedom in twins.

The tilt angles were measure in a 2 μm homogeneously aligned cell. The temperature dependence of the tilt angles is shown in figure 6 for ABPNP-10 and ABPNTP-10. The compound having a carboxylate linking group shows a higher tilt angle (*c*. 40°) than the compound containing the thioester group (*c*. 32°) at the same reduced temperature of 30°C.

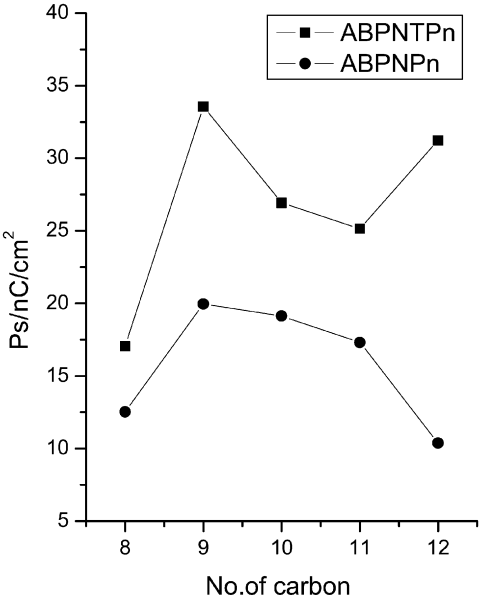

Figure 5. Spontaneous polarization of the ABPNP-*n* and ABPNTP-*n* series versus the achiral alkoxy chain length *n* at a constant reduced temperatures ($T-T_{SmA^*-SmC^*}=-20$°C).

4. Conclusion

We have synthesized two series of liquid crystalline twins having two identical chiral centers but linked with internal carboxylic or thioester groups. All the twins exhibit the SmC* phase. Mesomorphic investigation of the compounds shows the suppression of polymorphism on replacing the carboxylate linkage with a thioester linkage. It is also observed that the SmC* phase range is increased on increasing the achiral chain length in compounds containing a thioester linkage, whereas there is no significant change in compounds with a carboxylate linkage. In general, $\mathbf{P}_s$ value observed for thioester compounds were significantly larger than for the corresponding carboxylate analogues.

References

[1] Ober, C. K., Lin, J. I., and Lenz, R. W., 1984, *Adv. polym. Sci.*, **59,** 103.
[2] Griffin, A. C., and Britt, T. R., 1981, *J. Am. chem. Soc.*, **103,** 4957.

[3] IMRIE, C. T., and HENDERSON, P. A., 2002, *Curr. Opin. colloid inter. Sci.*, **7,** 298.
[4] KUMAR, P. A., and PISIPATI, V. G. K. M., 2000, *Adv. Mater.*, **12,** 1617.
[5] LE MASURIER, P. J., and LUCHURST, G. R., 1995, *Liq. Cryst.*, **25,** 63.
[6] NISHIYAMA, I., and YOSHIZAWA, A., 1994, *Liq. Cryst.*, **17,** 555.
[7] NASSIF, L., JAKLI, A., and SEED, A. J., 2001, *Mol. Cryst. liq. Cryst.*, **365,** 171.
[8] OKAMOTO, H., HAYASHI, M., and TAKENAKA, S., 1996, *Liq. Cryst.*, **20,** 647.
[9] NEUBERT, M. E., MERCHANT, B. Z., JIROUSEK, M. R., LASKOS JR, S. J., LEONHARDT, D., and SHARMA, R. B., 1998, *Mol. Cryst. liq. Cryst.*, **154,** 209.
[10] ROBINSON, W. K., CARBONI, C., KLOESS, P., PERKINS, S. P., and COLES, H. J., 1998, *Liq. Cryst.*, **25,** 301.
[11] BYRON, D. J., KOMITOV, L., MATHARU, A. S., MCSHERRY, I., and WILSON, R. C., 1996, *J. mater. Chem.*, **6,** 1871.
[12] SEED, A. J., HIRD, M., STYRING, P., GLEESON, H. F., and MILLS, J. T., 1997, *Mol. Cryst. liq. Cryst.*, **299,** 19.
[13] KELKER, H., and HATZ, R., 1980, *Hand Book of Liquid Crystals*, edited by C. Schumann (Verlag Chemie), p. 174.
[14] DABROWSKI, R., DZIADUSZEK, J., SZCZUCINSKI, T, and RASZEWSKI, Z., 1984, *Mol. Cryst. liq. Cryst.*, **107,** 411.
[15] DABROWSKI, R., DZIADUSZEK, J., and SZCZUCINSKI, T., 1985, *Mol. Cryst. liq. Cryst.*, **124,** 241.
[16] NISHIYAMA, I., YAMAMOTO, J., GOODBY, J. W., and YOKOYAMA, H., 2002, *Liq. Cryst.*, **29,** 1409.
[17] MIYASATO, K., ABE, S., TAKEZOE, H., FUKUDA, A., and KUZE, E., 1983, *Jpn. J. appl. Phys.*, **22,** L661.
[18] CHANDANI, A. D. L., HAGIWARA, T., SUZUKI, Y., OUCHI, Y., TAKAZOE, H., and FUKUDA, A., 1988, *Jpn. J. appl. Phys.*, **27,** L729.
[19] LEE, J., CHANDANI, A. D. L., ITOH, K., OUCHI, Y., TAKEZOE, H., and FUKUDA, A., 1990, *Jpn. J. appl. Phys.*, **29,** 1122.
[20] GRAY, G. W., and GOODBY, J. W., 1984, *Smectic Liquid Crystals-Textures and Structures* (USA: Leonard Hill).
[21] WU, S. L., CHEN, D. G., CHEN, S. J., WANG, C. Y., and SHY, J. T., 1995, *Mol. Cryst. liq. Cryst.*, **264,** 39.
[22] WU, S.-L., and HSIEH, W.-J., 1996, *Ferroelectrics*, **180,** 259.